Multipole expansion in plasmas: Effective interaction potentials between compound particles

T. S. Ramazanov,[1] Zh. A. Moldabekov,[1,*] and M. T. Gabdullin[1,2]
[1]*Institute for Experimental and Theoretical Physics, Al-Farabi Kazakh National University, 71, Al-Farabi Avenue, 050040, Almaty, Kazakhstan*
[2]*National Nanotechnology Laboratory of Open Type, Al-Farabi Kazakh National University, 71, Al-Farabi Avenue, 050040, Almaty, Kazakhstan*
(Received 24 February 2016; published 9 May 2016)

In this paper, the multipole expansion method is used to determine effective interaction potentials between particles in both classical dusty plasma and dense quantum plasma. In particular, formulas for interactions of dipole-dipole and charge-dipole pairs in a classical nondegenerate plasma as well as in degenerate quantum and semiclassical plasmas were derived. The potentials describe interactions between atoms, atoms and charged particles, dust particles in the complex plasma, atoms and electrons in the degenerate plasma, and metals. Correctness of the results obtained from the multipole expansion is confirmed by their agreement with the results based on other methods of statistical physics and dielectric response function. It is shown that the method of multipole expansion can be used to derive effective interaction potentials of compound particles, if the effect of the medium on the potential of individual particles comprising compound particles is known.

DOI: 10.1103/PhysRevE.93.053204

I. INTRODUCTION

Effective interaction potentials are widely used in many-particle physics. In particular, effective interaction potentials are used in analytical calculations and computer modeling in such areas as condensed matter physics [1–3], plasma physics [4–20], nuclear physics [21–23], physics of colloidal systems [24,25], molecular biophysics [26], as well as nanotechnology [27]. The use of effective potentials enables physicists to significantly simplify the problem and to get a clearer picture of the process, deepening its understanding [28–42]. The effective interaction potentials can be divided into two classes. The first class includes effective potentials adjusted to account for short-range effects at small distances such as quantum effects of diffraction and symmetry [43–49], and the finite particle size [24,50–52], without taking into account the collective effects. The second class includes effective interaction potentials, which also take into account many-particle collective effects such as screening [54–56]. In this paper we consider the effective interaction potentials belonging to the second class. The interaction potentials, not taking into account many-particle effects (the influence of the medium) are referred to as micropotentials. Various methods are used to obtain effective interaction potentials of the second class. It is necessary to mention that there are methods based on the kinetic equations [12,15,16,56] and the formalism of the dielectric response function [4,5,17–20]. However, these methods, though well substantiated and verified, require derivation of integrals and it is difficult to use them to find effective interaction potentials between compound particles such as dipoles, as the potentials of the latter do not have spherical symmetry, which makes it difficult, and often impossible, to find analytical formulas by integrating. In this paper, we show that the method of multipole expansion makes it easy to find effective interaction potentials between compound particles, if we know the effect of the medium on the potential of individual particles comprising compound particles. In this case, the problem of finding effective interaction potentials is reduced to the problem of finding derivatives of the function. This procedure will be shown below.

One of the plasma components is often ideal or weakly coupled, whereas the other component (consisting of relatively inert particles) creates a strongly coupled subsystem on the background of mobile weakly coupled particles. In the case of a complex plasma, dust particles create a strongly coupled subsystem where the interaction potential between dust particles is screened by weakly coupled ions and electrons. In the case of dense plasma or warm dense matter, ions can create a strongly correlated subsystem on the background of mobile weakly coupled electrons. In these cases, strongly correlated inert particles can be investigated via effective interparticle interaction potentials, where initially screening provided by mobile weakly coupled particles (electrons), whereas many-body effects due to strongly coupled species included naturally in simulations such as molecular dynamics or Monte Carlo. In the present work the screening effect in a complex (dusty) plasma as well as in dense plasma (warm dense matter) due to weakly coupled particles is considered.

In Sec. II the way to derive screened interaction potential between two compound particles using a multipole expansion of the potential of single particle in polarizable media is presented. First, in Sec. II A, the application of the multipole expansion to the system of charges interacting by Coulomb potential and review of known results are shortly given. In Sec. II B the interaction potentials between compound particles in the classical plasma taking into account screening effects are considered and discussed in connection with the application of these potentials for the study of a dusty plasma. In Sec. II C the effective potentials of dipole-charge and atom-charge interactions in the plasma with degenerate electrons are derived and discussed in connection with their application for the investigation of a partially ionized plasma and warm dense matter. At the end of the second section an effective long-ranged interaction potential between the electron and the

*zhandos@physics.kz

dipole (atom) in a degenerate plasma and in metals, taking into account so called Friedel oscillations, is derived.

II. INTERACTION POTENTIALS BETWEEN COMPOUND PARTICLES

Two systems of charged particles are considered, each of which consists of charges $e_i^{(\alpha)}$, where i indicates the number of the charge and the superscript α indicates that this charge belongs to the first ($\alpha = 1$) or second ($\alpha = 2$) system. At distances greater than the linear size of the system we expand the potential of the first system of charged particles using the following formula:

$$f(\mathbf{R}-\mathbf{r}) \simeq f(\mathbf{R}) - \mathbf{r}\cdot\nabla f(\mathbf{R}) + \cdots, \tag{1}$$

We denote the dipole moment $\mathbf{d}_\alpha = \sum e_i^{(\alpha)}\mathbf{r}_i^{(\alpha)}$ and the total charge $Q_\alpha = \sum e_i^{(\alpha)}$ of the system. The potential energy of interaction of the first system of charges with the second one, located at a distance $\mathbf{R}$ from the first, has the following form:

$$\Phi(\mathbf{R}) = \psi_1(\mathbf{R})Q_2 + \nabla\psi_1(\mathbf{R})\cdot\mathbf{d}_2 + \cdots, \tag{2}$$

where ψ_1 is the potential of the first system of charges at a distance $\mathbf{R}$,

$$\psi_1(\mathbf{R}) = \sum \phi_i\big(|\mathbf{R} - \mathbf{r}_i^{(\alpha)}|\big), \tag{3}$$

and ϕ_i is the potential of the charge $e_i^{(1)}$.

Below we show that the potential of a compound particle in a polarizable medium can be obtained from Eq. (2), starting from the potential of the single charge in this medium and using expansion Eq. (1) of the total potential ψ.

In a plasma the potential of an individual particle is determined by the formula

$$\phi(\mathbf{r}) = \int \frac{d\mathbf{k}}{2\pi^2}\frac{Q_i}{k^2\epsilon(\mathbf{k})}e^{i\mathbf{k}\cdot\mathbf{r}}, \tag{4}$$

where the screening is provided via a proper dielectric function ϵ (a schematic explanation is given in Fig. 1).

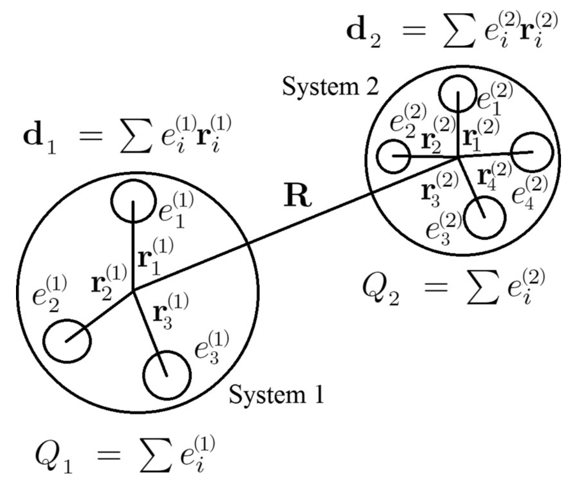

FIG. 1. A schematic explanation of calculations of the interaction energy of two compound systems (particles). Each system has an total charge $Q_\alpha = \sum e_i^{(\alpha)}$ and dipole moment $\mathbf{d}_\alpha = \sum e_i^{(\alpha)}\mathbf{r}_i^{(\alpha)}$, where α indicates that this charge belongs to the first ($\alpha = 1$) or second ($\alpha = 2$) system. Interaction potential between these two systems is considered on the basis of the multipole expansion taking the distance R greater than the linear size of the systems $R \gg \max(r_i^{(\alpha)})$.

A. Multipole expansion on the basis of Coulomb potential

To better understand further calculations using the multipole expansion, let us first shortly consider their application to the system of charges interacting by Coulomb potential and rederive some well-known results. If we take ϕ as Coulomb potential ($\epsilon = 1$), Eq. (2) gives a well-known result:

$$\Phi(\mathbf{R}) = \frac{Q_1Q_2}{R} + \frac{(Q_2\mathbf{d}_1 - Q_1\mathbf{d}_2)\cdot\mathbf{R}}{R^3} + \frac{(\mathbf{d}_1\cdot\mathbf{d}_2)R^2 - 3(\mathbf{d}_1\cdot\mathbf{R})(\mathbf{d}_2\cdot\mathbf{R})}{R^5}. \tag{5}$$

If $Q_2 = 0, d_1 = 0$, the charge-dipole interaction potential is equal to

$$\Phi_{\text{d-ch}}(\mathbf{R}) = -\frac{Q_1(\mathbf{d}_2\cdot\mathbf{R})}{R^3}. \tag{6}$$

Introducing the coefficient of atomic polarization $\bar{\alpha}$, from Eq. (6) we get a well-known formula for the interaction of an atom with a charged particle:

$$\Phi_{\text{a-ch}}(R) = -\frac{\bar{\alpha}Q_1^2}{2R^4}. \tag{7}$$

Usually, in calculations the cutoff radius r_c is used:

$$\Phi_{\text{a-ch}}(R) = -\frac{\bar{\alpha}Q_1^2}{2\big(R^2 + r_c^2\big)^2}. \tag{8}$$

for example, the cutoff radius for hydrogen is equal to $r_c = (\bar{\alpha}a_B/2)^{1/4}$ (here a_B is the first Bohr radius) [7,52].

From Eq. (5) for $Q_1 = 0, Q_2 = 0$ we can obtain the interaction potential of two dipoles:

$$\Phi(\mathbf{R}) = \frac{(\mathbf{d}_1\cdot\mathbf{d}_2)R^2 - 3(\mathbf{d}_1\cdot\mathbf{R})\cdot(\mathbf{d}_2\cdot\mathbf{R})}{R^5}, \tag{9}$$

To determine the interaction between two atoms it is necessary to average over the angles, using the Boltzmann factor. In this case three types of interactions are considered: the interaction between permanent dipoles (Debye interaction $\beta = 2/3d^4/(k_BT)$, where k_BT is atomic thermal energy), interaction of a permanent dipole with an induced dipole (Keesom interaction $\beta = \bar{\alpha}d^2$), and interaction between induced dipoles (London interaction $\beta = 3/4\bar{\alpha}^2I$, where I is the ionization potential of the atom). Using the potential Eq. (9), we obtain, after averaging over the angles, the energy of interaction between two atoms:

$$\Phi_{\text{a-a}}(R) = -\frac{\beta}{R^6}. \tag{10}$$

The interaction Eq. (10) occurs between any types of atoms.

B. Effective interaction potentials between compound particles in a classical plasma

For a classical plasma, we take the dielectric function in the following form:

$$\epsilon(k) = 1 + \frac{k_S^2}{k^2}, \tag{11}$$

where k_S is the inverse screening length.

According to Eq. (4), the dielectric function Eq. (11) gives screened Yukawa (Debye) potential of a charged particle in a classical plasma $\phi_i(r) = e_i/r \exp(-rk_S)$. Using expansion Eq. (1) of ψ_1, we get

$$\psi_1(\mathbf{R}) = \frac{Q_1}{R}\exp(-Rk_S) + \frac{\mathbf{d}_1 \cdot \mathbf{R}}{R^3}(1 + Rk_S)\exp(-Rk_S). \tag{12}$$

Substituting Eq. (12) to Eq. (2), we obtain

$$\begin{aligned}\Phi(\mathbf{R}) = {}& \frac{Q_1 Q_2}{R}\exp(-Rk_S) + \frac{(Q_2\mathbf{d}_1 - Q_1\mathbf{d}_2)\cdot\mathbf{R}}{R^3}(1 + Rk_S)\exp(-Rk_S)\\ &+ \frac{[(\mathbf{d}_1\cdot\mathbf{d}_2)R^2 - (\mathbf{d}_1\cdot\mathbf{R})\cdot(\mathbf{d}_2\cdot\mathbf{R})(3 + Rk_S)](1 + Rk_S) + (\mathbf{d}_1\cdot\mathbf{R})\cdot(\mathbf{d}_2\cdot\mathbf{R})Rk_S}{R^5}\exp(-Rk_S).\end{aligned} \tag{13}$$

Of special interest is the case when two compound particles have dipole moments parallel and equal to each other, $\mathbf{d}_1 \uparrow\uparrow \mathbf{d}_2$, and perpendicular to the radius vector $\mathbf{R}$, $\mathbf{d}_1 \cdot \mathbf{R} = \mathbf{d}_2 \cdot \mathbf{R} = 0$. For such particles Eq. (13) gives

$$\Phi(R) = \frac{Q^2}{R}\exp(-Rk_S) + \frac{d^2}{R^3}(1 + Rk_S)\exp(-Rk_S), \tag{14}$$

where $d = d_1 = d_2$ and $Q = Q_1 = Q_2$.

It has been shown that in a dusty plasma, due to the directional flow of ions in the area behind the negatively charged dust particle (with respect to the incident ion flux) a region with an excess concentration of ions is formed [57–60]. A negatively charged dust particle and a cloud of positive ions can be considered as a single-compound particle with a nonzero dipole moment and a nonzero total charge [60,61]. In the case when the dust particles are located on the same horizontal line perpendicular to the direction of the ion flow, the effective potential Eq. (14) describes the interaction of dust particles. As it can be seen, the effective potential Eq. (14) gives a stronger repulsion between the dust particles than the Yukawa potential. Recently, using Eq. (14) we have shown that even weak additional dipole-dipole interaction can lead to the dramatic changes in the static and dynamic properties of the system of dust particles [42,62]. We note that we give derivation of the potential Eq. (14) here for the first time.

There are systems with dominant Yukawa interaction and systems, in contrast, with dominant dipole-dipole interaction. Therefore, it is interesting to study dynamical and statical properties in intermediate cases, creating a bridge between the physics of strongly coupled Coulomb systems and the physics of systems with dipole interaction [63].

In case the dust particles are arranged along the direction of the ion flow, $\mathbf{d}_1 \cdot \mathbf{R} = \mathbf{d}_2 \cdot \mathbf{R} = dR$, from Eq. (13) we obtain

$$\begin{aligned}\Phi(R) = {}& \frac{Q^2}{R}\exp(-Rk_S)\\ &- \frac{2d^2}{R^3}\left(1 + Rk_S + \frac{R^2k_S^2}{2}\right)\exp(-Rk_S).\end{aligned} \tag{15}$$

In general, the charges of the dust particles can be different due to different sizes or the places of location in a plasma. In this case, interaction potential can be found from general Eq. (13). The dipole moment of the compound dust particle [charged dust particle + focused (or captured) ion cloud] can be determined by solving the kinetic equation for ions [60] or by comparison of the particles positions pair correlation function and velocities autocorrelation function obtained from the experiment with those obtained via molecular dynamics simulation [42,64].

Now, let us consider a charge-dipole interaction, $Q_2 = 0, d_1 = 0$. From Eq. (13) we obtain

$$\Phi_{\text{d-ch}}(\mathbf{R}) = -\frac{Q_1(\mathbf{d}_2\cdot\mathbf{R})}{R^3}(1 + Rk_S)\exp(-Rk_S). \tag{16}$$

Using the coefficient of polarizability of the atom $\bar{\alpha}$, we obtain the following formula for the interaction of an atom with a charged particle:

$$\Phi_{\text{a-ch}}(R) = -\frac{\bar{\alpha}Q_1^2}{2R^4}(1 + Rk_S)^2\exp(-2Rk_S). \tag{17}$$

Introducing the cutoff length r_c, we can get the well-known Buckingham screened potential [8,52,53]:

$$\Phi_{\text{a-ch}}(R) = -\frac{\bar{\alpha}Q_1^2}{2\left(R^2 + r_c^2\right)^2}(1 + Rk_S)^2\exp(-2Rk_S). \tag{18}$$

This result confirms the correctness of using of multipole expansion of potential Eq. (4).

Let us consider the interaction of two compound particles with nonzero dipole moments, but with zero total charges $Q_1 = Q_2 = 0$. From Eq. (13) we obtain

$$\begin{aligned}\Phi(\mathbf{R}) = {}& \frac{1}{R^5}[[(\mathbf{d}_1\cdot\mathbf{d}_2)R^2 - (\mathbf{d}_1\cdot\mathbf{R})\cdot(\mathbf{d}_2\cdot\mathbf{R})(3 + Rk_S)]\\ &\times(1 + Rk_S) + (\mathbf{d}_1\cdot\mathbf{R})\cdot(\mathbf{d}_2\cdot\mathbf{R})Rk_S]\exp(-Rk_S).\end{aligned} \tag{19}$$

In order to define the interaction between two atoms it is necessary to make averaging over the angles in Eq. (19). After averaging over the angles with the Boltzmann factor, we get the following formula for the effective interaction potential between atoms:

$$\Phi_{\text{a-a}}(R) = -\frac{\beta}{R^6}\left(1 + Rk_S + \frac{R^2k_S^2}{2}\right)^2\exp(-2Rk_S). \tag{20}$$

The screened potential Eq. (20) describes the attraction part of interatomic interactions.

C. Effective interaction potentials between compound particles in a quantum plasma

We start from the recently obtained expansion of the inverse value of the Lindhard dielectric function of electrons in the long wavelength limit [14]. The second-order result of this expansion has the following form:

$$\epsilon_2^{-1}(\mathbf{k},0) = \frac{k^2\left(1+\frac{\tilde{a}_2}{\tilde{a}_0}k^2\right)}{k^2+\kappa_Y^2+\frac{\tilde{a}_2}{\tilde{a}_0}k^4}. \tag{21}$$

The result for $\tilde{a}_2/\tilde{a}_0$ is

$$\frac{\tilde{a}_2}{\tilde{a}_0} = \frac{I_{-3/2}(\gamma_0)}{12\theta k_F^2 I_{-1/2}^2(\gamma_0)}. \tag{22}$$

Here, $k_F = (3\pi^2 n)^{1/3}$, I_ν is the Fermi integral of order ν, $\gamma_0 = \mu/k_BT$ is the chemical potential of electrons, $k_Y^2 = k_{TF}^2\theta^{1/2}I_{-1/2}(\gamma_0)/2$ is the screening length, which interpolates between Debye and Thomas-Fermi expansions, and $\theta = k_BT/E_F$ is the degeneracy parameter, which defines whether plasma is degenerate or classical. The electron density is characterized by the density parameter $r_S = a/a_B$, where $a = (4/3\pi n)^{-1/3}$ and a_B is the first Bohr radius. This dielectric function takes into account the first-order gradient correction to the noninteracting kinetic energy of electrons [14].

The dielectric function Eq. (21) was obtained by expanding electrons' polarization function $\Pi_e(\mathbf{k})$ and neglecting contribution of ions to the dielectric function, $\Pi_{\text{ion}} = 0$. If we take into account the contribution of ions to the dielectric function, the following equation for the inverse value of the dielectric function can be obtained [4]:

$$\epsilon_2(\mathbf{k})^{-1} = \frac{k^2\left(1+\frac{\tilde{a}_2}{\tilde{a}_0}k^2\right)}{k^2\left(1+\frac{\tilde{a}_2}{\tilde{a}_0}k_{Di}^2\right)+k_D^2+\frac{\tilde{a}_2}{\tilde{a}_0}k^4}, \tag{23}$$

where $k_D^2 = k_Y^2 + k_{Di}^2$ and $k_{Di}^2 = 4\pi n_i e^2/k_BT_i$.

The dielectric function Eq. (23) was derived taking into account a classical long-wavelength limit of the ions' polarization function in random phase approximation $\Pi_{\text{ion}}(\mathbf{k}) = -n_{\text{ion}}/(k_BT_{\text{ion}})$. Equation (23) turns into Eq. (21) if we take $k_{Di} = 0$.

Using the dielectric function Eq. (23), we find the potential of the system of charged particles,

$$\psi_1(\mathbf{R}) = \frac{Q_1}{R}f_1(R) + \frac{\mathbf{d}_1\cdot\mathbf{R}}{R^3}f_2(R), \tag{24}$$

and the energy of interaction between two compound particles in a quantum plasma,

$$\Phi(\mathbf{R}) = \frac{Q_1Q_2}{R}f_1(R) + \frac{(Q_2\mathbf{d}_1 - Q_1\mathbf{d}_2)\cdot\mathbf{R}}{R^3}f_2(R) + \frac{(\mathbf{d}_1\cdot\mathbf{d}_2)R^2 - 3(\mathbf{d}_1\cdot\mathbf{R})\cdot(\mathbf{d}_2\cdot\mathbf{R})}{R^5}f_3(R), \tag{25}$$

where for convenience we introduced the following exponential functions and constant coefficients:

$$\begin{aligned}
f_1(R) &= \frac{1}{\gamma^2\sqrt{1-(2k_D/\lambda\gamma^2)^2}}\left[\left(\frac{1}{\lambda^2}-B^2\right)\exp(-RB) - \left(\frac{1}{\lambda^2}-A^2\right)\exp(-RA)\right],\\
f_2(R) &= \frac{1}{\gamma^2\sqrt{1-(2k_D/\lambda\gamma^2)^2}}\left[\left(\frac{1}{\lambda^2}-B^2\right)(1+RB)\exp(-RB) - \left(\frac{1}{\lambda^2}-A^2\right)(1+RA)\exp(-RA)\right],\\
f_3(R) &= \frac{1}{\gamma^2\sqrt{1-(2k_D/\lambda\gamma^2)^2}}\left[3\left(\frac{1}{\lambda^2}-B^2\right)(1+RB)\exp(-RB) + \left(\frac{1}{\lambda^2}-B^2\right)B^2R^2\exp(-RB)\right.\\
&\quad\left. - 3\left(\frac{1}{\lambda^2}-A^2\right)(1+RA)\exp(-RA) - \left(\frac{1}{\lambda^2}-A^2\right)A^2R^2\exp(-RA)\right].
\end{aligned} \tag{26}$$

Here, $\lambda^2 = \tilde{a}_2/\tilde{a}_0$, $\gamma^2 = 1/\lambda^2 + k_{Di}^2$, $A^2 = \frac{\gamma^2}{2}[1+\sqrt{1-(\frac{2k_D}{\lambda\gamma^2})^2}]$, and $B^2 = \frac{\gamma^2}{2}[1-\sqrt{1-(\frac{2k_D}{\lambda\gamma^2})^2}]$.

Using the polarizability coefficient of the atom and the cutoff length, we obtain the following formula for the interaction of the atom with a charged particle in a plasma with degenerate electrons:

$$\Phi_{\text{a-ch}}(R) = -\frac{\bar{\alpha}Q_1^2}{2(R^2+r_c^2)^2}\times[f_2(R)]^2. \tag{27}$$

In Fig. 2 the comparison of the derived potential Eq. (27) with the screened Buckingham potential Eq. (18) is given. As it is seen, electron degeneracy leads to weakening of screening of the atomic potential.

Weakening of screening is due to the inclusion of the so-called quantum diffraction effect or, according to Dunn and Broyles [45], it is a result of the quantum tunneling effect, which allows particles to reach regions inaccessible for classical particles. This effect is characterized by the coefficient $\lambda = \sqrt{\tilde{a}_2/\tilde{a}_0}$.

In order to demonstrate the importance of the quantum diffraction effect for accurate calculations of transport and thermodynamic properties of a dense plasma and warm dense matter, in Fig. 3 we present the results of calculation of the s-wave scattering phase shifts for electron-atom scattering. The determination of the values of phase shifts at $R\to\infty$ is a starting point for investigation of the plasma properties [7,8,30,34]. As it is seen from Fig. 3, even at weak degeneracy $\theta \leqslant 2$ the quantum diffraction effect is important. For $\theta \leqslant 0.5$, this effect can increase the value of the phase shift up to 30%. At large values of θ, as it is expected, the quantum diffraction effect can be neglected.

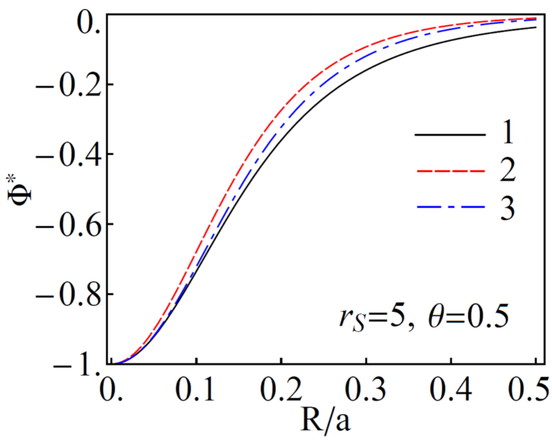

FIG. 2. Electron-atom interaction potentials for hydrogen plasma at $r_S = 5, \theta = 0.5$: 1, micropotential (8); 2, screened Buckingham potential Eq. (18) with $k_S = k_Y$; 3, screened potential Eq. (27). The values of potentials are given in dimensionless units $\Phi^* = \Phi/(\bar{\alpha}e^2/r_c^4)$. For hydrogen $r_c = (\bar{\alpha}a_B/2)^{1/4}$ and $\bar{\alpha} = 4.5a_B^3$.

In Tables I–III, the values of the electron-hydrogen atom scattering phase shifts (s-wave) obtained using the screened Buckingham potential Eq. (18) with $k_S = k_Y$ and the potential Eq. (27) for different values of the degeneracy parameter θ at the wave number $\kappa = 0.8a_B^{-1}$ and the density parameters $r_S = 5$, $r_S = 3$, and $r_S = 10$ are presented. The phase shifts were calculated solving the Calogero equation. The values of relative difference in the phase shifts clearly indicate that the quantum diffraction effect is important for high-density $r_S = 3$ as well as for low-density $r_S = 10$ cases. As only the impact of the quantum diffraction effect on the interparticle interaction potential is investigated, the plasma temperature and concentration are taken as independent parameters.

After averaging over the angles with the Boltzmann factor, from Eq. (25) we obtain the attraction part of the effective

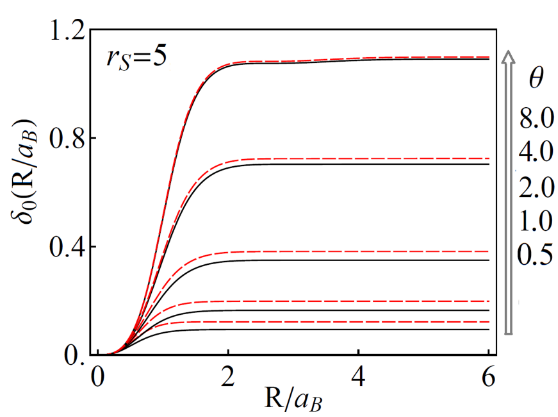

FIG. 3. Electron-hydrogen atom scattering phase shifts (s-wave) obtained using the screened Buckingham potential Eq. (18) with $k_S = k_Y$ (solid lines) and the potential Eq. (27) (dash lines) as a function of distance for different values of the degeneracy parameter θ at the wave number $\kappa = 0.8a_B^{-1}$ and the density parameter $r_S = 5$. The phase shifts were calculated solving the Calogero equation.

TABLE I. Electron-hydrogen atom scattering phase shifts (s-wave) at $r_S = 5$. Here δ_0' is the phase shift obtained using the screened Buckingham potential Eq. (18) with $k_S = k_Y$, and δ_0'' is the phase shift obtained using the potential Eq. (27).

θ	0.5	1.0	2.0	4.0	8.0
δ_0'	0.094	0.164	0.35	0.7	1.091
δ_0''	0.122	0.198	0.38	0.72	1.098
$\frac{\delta_0''-\delta_0'}{\delta_0'} \times 100$	30%	21%	8.6%	2%	0.6%

interaction potential between atoms:

$$\Phi_{\text{a-a}}(R) = -\frac{\beta}{\gamma^4(1-(2k_D/\lambda\gamma^2)^2)R^6} \times \left[\left(1+RB+\frac{R^2B^2}{2}\right)^2\left(\frac{1}{\lambda^2}-B^2\right)^2\exp(-2BR) - \left(1+RA+\frac{R^2A^2}{2}\right)^2\left(\frac{1}{\lambda^2}-A^2\right)^2\exp(-2AR)\right]. \tag{28}$$

In Fig. 4 the comparison of the derived potential Eq. (28) with the screened potential Eq. (20) is given. As in the case of charge-atom interaction considered above, the electron degeneracy leads to a weakening of screening in comparison with the case when the quantum diffraction effect is neglected ($\lambda = 0$).

At $\lambda = 0$, the effective potential Eq. (28) turns into the effective potential Eq. (20), which does not take into account the wave nature of plasma electrons. Hence, at $\lambda = 0$ the effective potential Eqs. (27) and (25) turn into Eqs. (18) and (13), respectively. In Eq. (4) the Fourier transform of the charge potential is defined as the ratio of the Fourier transform of the Coulomb potential to the static dielectric function. If we define this potential as the ratio of the Fourier transform of the quantum Deutsch potential [46] to the static dielectric function Eq. (23), but without ion contribution and with semiclassical electrons ($\lambda = \hbar/\sqrt{\pi m_e k_B T}$), and make multipole expansion, we obtain an expression for the effective interaction potential between an atom and a charge, which exactly corresponds to the result obtained in Ref. [18] by the methods of statistical physics [65]. This, again, confirms the validity of the method used in this work.

D. Friedel oscillations generated by a dipole or atom

In a fully degenerate plasma, electrons obey Fermi-Dirac statistics. In such a plasma the potential around the charge in addition to the exponentially decreasing term (considered above) has a long-range oscillating term. The latter term is

TABLE II. The same as in Table I but at $r_S = 3$.

θ	0.5	1.0	2.0	4.0	8.0
δ_0'	0.089	0.154	0.319	0.634	0.994
δ_0''	0.117	0.186	0.349	0.654	1.002
$\frac{\delta_0''-\delta_0'}{\delta_0'} \times 100$	31%	21%	9.4%	3%	0.8%

TABLE III. The same as in Table I but at $r_S = 10$.

θ	0.5	1.0	2.0	4.0	8.0
δ_0'	0.096	0.170	0.365	0.738	1.142
δ_0''	0.124	0.203	0.398	0.759	1.149
$\frac{\delta_0''-\delta_0'}{\delta_0'}\times 100$	29%	19.4%	9%	2.8%	0.6%

known as Friedel oscillations. At long distances from the charged particle the potential oscillations have the following form [66]:

$$\phi_i(r) = -\frac{e_i\lambda_{\mathrm{TF}}^2 36\gamma_0^4}{\left(2+3\gamma_0^2\right)^2}\frac{\cos(2k_F r)}{r^3}, \tag{29}$$

where λ_{TF} is the Thomas-Fermi radius, $\gamma_0 = \hbar\omega_p/E_F$ is the coupling parameter in the quantum plasma, ω_p is the plasma frequency, and E_F is the Fermi energy. The potential Eq. (29) can be obtained from Eq. (4) using the Lindhard dielectric function. Now, starting from Eq. (3) with account for Eq. (29), and expanding it using Eq. (1) in accordance with Eq. (2) for the electron-dipole interaction, we obtain the following expression:

$$\Phi_{\text{e-d}}(\mathbf{R}) = -\frac{\lambda_{TF}^2 36\gamma_0^4 e}{\left(2+3\gamma_0^2\right)^2} \times \frac{\mathbf{d}\cdot\mathbf{R}}{R^4}\left[2k_F\sin(2k_F R) - \frac{3\cos(2k_F R)}{R}\right], \tag{30}$$

where e is the electron charge.

From Eq. (30) we get the following formula for the atom-electron interaction:

$$\Phi_{\text{e-a}}(R) = -\left[\frac{\lambda_{\mathrm{TF}}^2 36\gamma_0^4}{\left(2+3\gamma_0^2\right)^2}\right]^2 \times \frac{e^2\bar{\alpha}}{R^6}\left[2k_F\sin(2k_F R) - \frac{3\cos(2k_F R)}{R}\right]^2. \tag{31}$$

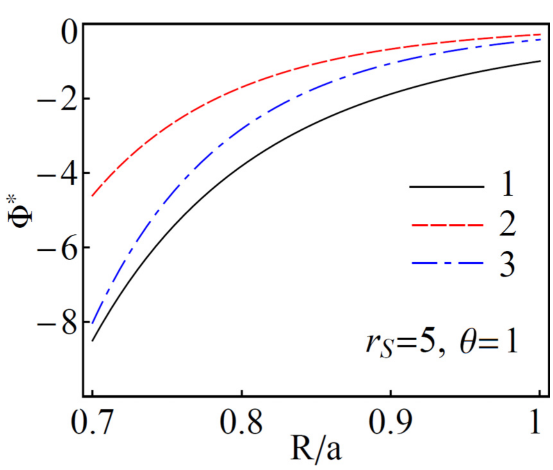

FIG. 4. The attraction part of atom-atom interaction potentials at $r_S = 5, \theta = 1$. 1, micro-potential Eq. (10); 2, screened Buckingham potential Eq. (20); 3, screened potential Eq. (28). The values of the potentials are given in dimensionless units $\Phi^* = \Phi/(\beta/a^6)$.

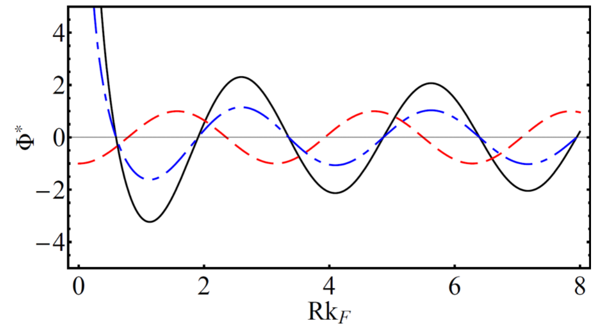

FIG. 5. The dipole potential in quantum plasma Eq. (30). The solid curve corresponds to $\mathbf{d}\frac{\mathbf{R}}{R} = 1$, the dashed-dotted curve corresponds to $\mathbf{d}\frac{\mathbf{R}}{R} = 0.5$, and the dashed curve corresponds to potential Eq. (29). For illustration purposes, the dimensionless potential value multiplied by cubic distance is given, $\Phi^* = \Phi \times R^3(e_i\lambda_{\mathrm{TF}}^2 36\gamma_0^4/(2+3\gamma_0^2)^2)^{-1}$.

If the second term in brackets in Eq. (30) at large distances is neglected, the dipole potential in the quantum system of degenerate electrons has the asymptotic form $\sim\sin(2k_F R)/R^3$. Thus, the potential of the dipole surrounded by degenerate electrons has the same asymptotic behavior as the potential of the charge; i.e., $\sim\cos(2k_F R)/R^3$. This is clearly seen from Fig. 5. However, the dipole potential has a cylindrical symmetry but not a spherical one. The dipole potential has its maximum along the direction of the dipole moment, as it is illustrated in Fig. 6(a).

In the case when the atom does not have permanent dipole moment, its potential decreases much faster than the potential Eq. (29). If we ignore the second term in the brackets of Eq. (31), we obtain the asymptotic behavior of the potential of the atom $\sim\sin(2k_F R)/R^6$. The effective potential Eq. (29) has spherical symmetry and is always negative [see Fig. 6(b)].

At large enough distances, where interaction due to atom polarization or permanent dipole moment is totally screened, the interaction potential Eqs. (31) and (30) are dominant. In contrast, in plasma, at small interparticle distances, the Friedel oscillations can be neglected [14].

At finite temperature, Friedel oscillations have the form $\cos(2k_F r)/r^2\exp(-wr)$, where $w = \sqrt{2m}\pi k_B T/\sqrt{\mu}\hbar$ [67] and can be neglected at $\theta > 1$ [14].

III. SUMMARY AND OUTLOOK

In the present study, the multipole expansion method was applied for the cases when the potential of a single charged particle in the studied medium is known. On the basis of this method, the effective interaction potentials of compound particles were obtained. Taking into account the screening of potentials of charges and wave nature of electrons, the effective interaction potentials for dipole-charge, dipole-dipole, charge-atom, and atom-atom pairs were derived.

The resulting effective interaction potentials describe the interaction of particles in a dusty plasma, in a partially ionized plasma, and in warm dense matter. In the case of a plasma with partially or fully degenerate electrons, from the viewpoint of the density functional theory, the dielectric function Eqs. (21) and (23) and the effective interaction potential Eqs. (24)–(28) take into account the contribution of the first-order gradient

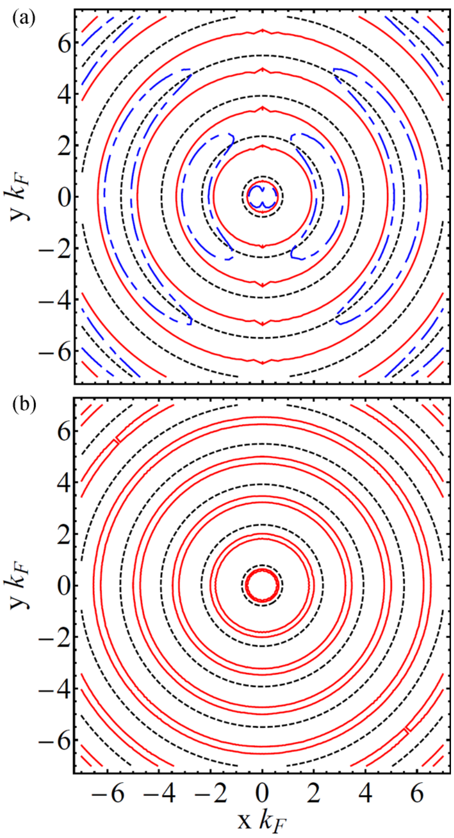

FIG. 6. (a) The contours of the dipole potential in quantum plasma Eq. (30), $\Phi^* = \Phi \times R^3[e_i\lambda_{\mathrm{TF}}^2 36\gamma_0^4/(2+3\gamma_0^2)^2]^{-1}$. The solid curve corresponds to $\Phi* = 0$, the dashed-dotted curve corresponds to $\Phi* = 0.1$, and the dotted curve corresponds to zero values of potential Eq. (29); (b) The contours of the atom potential in quantum plasma Eq. (31), $\Phi^* = \Phi \times R^6/(e^2\bar{\alpha})[e_i\lambda_{\mathrm{TF}}^2 36\gamma_0^4/(2+3\gamma_0^2)^2]^{-2}$. The solid curve corresponds to $\Phi* = -0.35$ and the dotted curve corresponds to zero values of potential Eq. (29). The atom (dipole) located at $(x = 0, y = 0)$.

correction of the noninteracting electrons kinetic energy to the free energy [14].

The effective screened dipole-electron and atom-electron interaction potentials were obtained. It was established that in quantum plasmas the asymptotic form of the dipole potential is the same as the form of the potential of a charged particle.

Effective interaction potentials between compound particles derived using the multipole expansion need extra information about the properties of considered compound particles. This information is incorporated in the dipole moment (permanent or induced). Once this dipole moment of the compound particle under consideration is obtained, the derived interaction potentials give a simple way to describe interaction between particles.

In the case of a charged dust particle in a plasma, the dipole moment can appear as a result of the dust particle polarization in the external field or as a result of the ion stream. The dipole moment of the dust grain can be obtained by solving the kinetic equation for ions and electrons near the dust particle surface [60,68] or by comparison of the experimentally obtained correlation functions for the dust particles system with those obtained from molecular dynamics simulation [42,64].

In the case of interaction of an atom with a charged particle or with another atom, the atom polarization coefficients $(\bar{\alpha}, \beta)$ can be obtained from quantum transition matrix elements of the given atom [69].

In polarizable medium such as plasma, the screening effect can significantly affect on the microscopic processes such as scattering, coagulation, etc. [70–74]. It was shown that the modification of the charge screening due to quantum diffraction effect should be taken into account for accurate calculations of the plasma properties. For generality, we included screening due to ions, but in a dense plasma (warm dense matter) the polarization function of ions in RPA can be inapplicable, because of strong nonideality of ions subsystem. In this case, one should put $k_i = 0$ in Eqs. (24)–(28), keeping screening due to electrons $k_e \neq 0$. Many-body correlation effects due to a nonideal subsystem of ions can be included using hypernetted chain approximation or molecular dynamics simulation. It is worth noting that in the case of moderate coupling between ions, the many-body effects due to ions can be included by an appropriate choice of the inverse screening length k_i, as it was recently shown by Stanton and Murillo [75].

Here we have proved that for interaction between compound particles the screening effect can be taken into account by, first, obtaining the potential of a single charge in the medium then further expanding this potential. In the case when higher-order terms of the multipole expansion are important, they can be obtained analytically for both classical and quantum plasmas from Eq. (2).

Derived potentials are relevant to (i) the complex (dusty) plasmas, where ions and electrons have number density of the order of $10^{10}\,\mathrm{cm}^{-3}$ and temperatures ∼300 K and $\sim 10^3$ K, respectively, and (ii) dense plasmas (warm dense matter), where plasma density $n > 10^{21}\,\mathrm{cm}^{-3}$ and temperature $T > 10^3$ K. In both cases the species that provides screening has to be weakly coupled.

In the case of stationary flowing plasma with a low streaming velocity the effect of dynamic screening can be included by modifying the screening length k_S as it was suggested by Kremp *et al.* [76] and Zwicknagel *et al.* [77] for an ideal plasma. Incorporation of the finite velocity effect leads to the weakening of the screening at higher velocities, as the screening background is unable to respond fast enough. As shown by Grabowski *et al.* [78], the following modification of the inverse screening length yields surprisingly good agreement when predicting dynamical properties $k_S(v) = k_S/(1+(v/v_{\mathrm{th}})^2)^{1/2}$, where $v_{\mathrm{th}} = (2k_B T/m)^{1/2}$ is the thermal velocity. However, in the case of highly nonequilibrium plasma with a high streaming velocity this procedure cannot be used. For such systems the effective dynamic potential has strong oscillations with deep minima and maximums, which can lead to attraction between like charged particles [5]. For a more detailed comparison of the nonrelativistic and ultrarelativistic cases, see Ref. [13]. The dynamic screening effect can have a strong influence on both structure properties [57] and dynamic properties [59,79] of the strongly coupled plasma.

ACKNOWLEDGMENT

This work has been supported by the Ministry of Education and Science of Kazakhstan under Grant No. F.0755 2016 (P.S.F.).

[1] Warren E. Pickett, Pseudopotential methods in condensed matter applications, Comput. Phys. Rep. **9**, 115 (1989).
[2] D. S. Petrov, G. E. Astrakharchik, D. J. Papoular, C. Salomon, and G. V. Shlyapnikov, Crystalline Phase of Strongly Interacting Fermi Mixtures, Phys. Rev. Lett. **99**, 130407 (2007).
[3] V. S. Filinov, V. E. Fortov, M. Bonitz, and Zh. Moldabekov, Fermionic path-integral Monte Carlo results for the uniform electron gas at finite temperature, Phys. Rev. E **91**, 033108 (2015).
[4] T. S. Ramazanov, Zh. A. Moldabekov, and M. T. Gabdullin, Effective potentials of interactions and thermodynamic properties of a nonideal two-temperature dense plasma, Phys. Rev. E **92**, 023104 (2015).
[5] Zh. A. Moldabekov, P. Ludwig, M. Bonitz, and T. S. Ramazanov, Ion potential in warm dense matter: Wake effects due to streaming degenerate electrons, Phys. Rev. E **91**, 023102 (2015).
[6] K. Weunsch, P. Hilse, M. Schlanges, and D. O. Gericke, Structure of strongly coupled multicomponent plasmas, Phys. Rev. E **77**, 056404 (2008).
[7] Y. A. Omarbakiyeva, C. Fortmann, T. S. Ramazanov, and G. Röpke, Cluster virial expansion for the equation of state of partially ionized hydrogen plasma, Phys. Rev. E **82**, 026407 (2010).
[8] Y. A. Omarbakiyeva, H. Reinholz, and G. Röpke, Cluster virial expansion of the equation of state for hydrogen plasma with e-H_2 contributions, Phys. Rev. E **91**, 043103 (2015).
[9] Sergey A. Khrapak and Hubertus M. Thomas, Practical expressions for the internal energy and pressure of Yukawa fluids, Phys. Rev. E **91**, 023108 (2015).
[10] C. E. Starrett and D. Saumon, Electronic and ionic structures of warm and hot dense matter, Phys. Rev. E **87**, 013104 (2013).
[11] C. E. Starrett and D. Saumon, A simple method for determining the ionic structure of warm dense matter, High Energy Density Phys. **10**, 35 (2014).
[12] Yu. V. Arkhipov, F. B. Baimbetov, and A. E. Davletov, Self-consistent chemical model of partially ionized plasmas, Phys. Rev. E **83**, 016405 (2011).
[13] Zh. A. Moldabekov, P. Ludwig, J. P. Joost, M. Bonitz, and T. Ramazanov, Dynamical screening and wake effects in classical, quantum, and ultrarelativistic plasmas, Contrib. Plasma Phys. **55**, 186 (2015).
[14] Zhandos Moldabekov, Tim Schoof, Patrick Ludwig, Michael Bonitz, and Tlekkabul Ramazanov, Statically screened ion potential and Bohm potential in a quantum plasma, Phys. Plasmas **22**, 102104 (2015).
[15] F. B. Baimbetov, M. A. Bekenov, and T. S. Ramazanov, Effective potential of a semiclassical hydrogen plasma, Phys. Lett. A **197**, 157 (1995).
[16] F. B. Baimbetov, Kh. T. Nurekenov, and T. S. Ramazanov, Pseudopotential theory of classical nonideal plasmas, Phys. Lett. A **202**, 211 (1995).
[17] T. S. Ramazanov and K. N. Dzhumagulova, Effective screened potentials of strongly coupled semiclassical plasma, Phys. Plasmas **9**, 3758 (2002).
[18] T. S. Ramazanov, K. N. Dzhumagulova, and Y. A. Omarbakiyeva, Effective polarization interaction potential charge-atom for partially ionized dense plasma, Phys. Plasmas **12**, 092702 (2005).
[19] T. S. Ramazanov, K. N. Dzhumagulova, and M. T. Gabdullin, Effective potentials for ion-ion and charge-atom interactions of dense semiclassical plasma, Phys. Plasmas **17**, 042703 (2010).
[20] T. S Ramazanov, Zh. A. Moldabekov, K. N. Dzhumagulova, and M. M. Muratov, Pseudopotentials of the particles interactions in complex plasmas, Phys. Plasmas **18**, 103705 (2011).
[21] Janaki Balakrishnan and Ian G. Moss, Improved effective potential, Phys. Rev. D **49**, 4113 (1994).
[22] Yasuo Kato and Noboru Takigawa, Effects of nonlinear screening and quantum motion of the target nucleus on low energy nuclear reactions in matter, Phys. Rev. C **76**, 014615 (2007).
[23] K. M. Udayanandan, P. Sethumadhavan, and V. M. Bannur, Equation of state of a quark-gluon plasma using the Cornell potential, Phys. Rev. C **76**, 044908 (2007).
[24] M. Majka and P. F. Gora, Analytical theory of effective interactions in binary colloidal systems of soft particles, Phys. Rev. E **90**, 032303 (2014).
[25] C. N. Likos, Effective interactions in soft condensed matter physics, Phys. Rep. **348**, 267 (2001).
[26] D. Marenduzzo, K. Finan, and P. R. Cook, The depletion attraction: an underappreciated force driving cellular organization, J. Cell. Biol. **175**, 681 (2006).
[27] H. Dietsch, V. Malik, M. Reufer, C. Dagallier, A. Shalkevich, M. Saric, T. Gibaud, F. Cardinaux, F. Scheffold, A. Stradner, and P. Schurtenberger, Soft nanotechnology from colloid physics to nanostructured functional materials, Chimia **62**, 805 (2008).
[28] T. S. Ramazanov, M. T. Gabdullin, K. N. Dzhumagulova, and R. Redmer, Ionization equilibrium and composition of a dense partially ionized metal plasma, Contrib. Plasma Phys. **51**, 391 (2011).
[29] M. T. Gabdullin, T. S. Ramazanov, and K. N. Dzhumagulova, Composition and thermodynamic properties of dense alkali metal plasmas, Contrib. Plasma Phys. **52**, 174 (2012).
[30] T. S. Ramazanov, K. N. Dzhumagulova, and A. Zh. Akbarov, Cross sections and transport coefficients of dense partially ionized semiclassical plasma, J. Phys. A: Math. Gen. **39**, 4335 (2006).
[31] T. S. Ramazanov, K. N. Dzhumagulova, and M. T. Gabdullin, Microscopic and thermodynamic properties of dense semiclassical partially ionized hydrogen plasma, J. Phys. A: Math. Gen. **39**, 4469 (2006).
[32] T. S. Ramazanov, K. N. Dzhumagulova, M. T. Gabdullin, A. Zh. Akbar, and R. Redmer, A scattering cross-section and ionization equilibrium in dense metal plasmas, J. Phys. A: Math. Theor. **42**, 214049 (2009).
[33] M.-Y. Song and Y.-D. Jung, Quantum screening effects on the electron-ion occurrence scattering time advance in strongly coupled semiclassical plasmas, Phys. Plasmas **10**, 3051 (2003).
[34] H.-M. Kim and Y.-D. Jung, Quantum effects on polarization transport scatterings in partially ionized dense hydrogen plasmas, Phys. Plasmas **14**, 074501 (2007).
[35] D.-H. Ki and Y.-D. Jung, Quantum screening effects on the ion-ion collisions in strongly coupled semiclassical plasmas, Phys. Plasmas **17**, 074506 (2010).
[36] D.-H. Ki and Y.-D. Jung, Formation of negative hydrogen ion: Polarization electron capture and nonthermal shielding, J. Chem. Phys. **137**, 094310 (2012).

[37] D.-H. Ki and Y.-D. Jung, Influence of non-thermal shielding on the Ramsauer phenomena for the electronatom-induced dipole scattering in Lorentzian plasmas, J. Plasma Phys. **79**, 113 (2013).
[38] S. K. Kodanova, T. S. Ramazanov, N. Kh. Bastykova, and Zh. A. Moldabekov, Effect of dust particle polarization on scattering processes in complex plasmas, Phys. Plasmas **22**, 063703 (2015).
[39] S. K. Kodanova, T. S. Ramazanov, M. K. Issanova, G. N. Nigmetova, and Zh. A. Moldabekov, Investigation of Coulomb logarithm and relaxation processes in dense plasma on the basis of effective potentials, Contrib. Plasma Phys. **55**, 271 (2015).
[40] T. S. Ramazanov, S. K. Kodanova, Zh. A. Moldabekov, and M. K. Issanova, Dynamical properties of nonideal plasma on the basis of effective potentials, Phys. Plasmas **20**, 112702 (2013).
[41] T. S. Ramazanov, Zh. A. Moldabekov, M. T. Gabdullin, and T. N. Ismagambetova, Interaction potentials and thermodynamic properties of two component semiclassical plasma, Phys. Plasmas **21**, 012706 (2014).
[42] Tlekkabul S. Ramazanov, Ayatola Zh. Gabdulin, and Zhandos A. Moldabekov, MD simulation of charged dust particles with dipole moments, IEEE Trans. Plasma Sci. **43**, 4187 (2015).
[43] A. E. Glauberman and I. R. Yukhnovskii, Dokl. Akad. Nauk SSSR **93**, 999 (1955); English translation: University of California Radiation Laboratory UCRL transl. 668(L) (unpublished).
[44] G. Kelbg, Theorie des Quantenplasmas, Ann. Phys. (Leipzig) **467**, 219 (1963).
[45] T. Dunn and A. A. Broyles, Method for determining the thermodynamic properties of the quantum electron gas, Phys. Rev. **157**, 156 (1967).
[46] C. Deutsch, Nodal expansion in a real matter plasma, Phys. Lett. A **60**, 317 (1977).
[47] H. Rahal, C. Deutsch, and M. M. Gombert, Temperature-dependent quantum pair potentials and ionization in helium-like plasmas, Contrib. Plasma Phys. **53**, 285 (2013).
[48] A. V. Filinov, M. Bonitz, and W. Ebeling, Improved Kelbg potential for correlated Coulomb systems, J. Phys. A: Math. Gen. **36**, 5957 (2003).
[49] Zh. A. Moldabekov, T. S. Ramazanov, and K. N. Dzhumagulova, Pair interaction potential of particles for two-component plasma, Contrib. Plasma Phys. **52**, 207 (2012).
[50] F. Palumbo, Effective interaction and effective operators with hard-core potentials, Phys. Rev. C **4**, 327 (1971).
[51] M. Natapoff, Pseudopotentials and the radius of the atomic core, J. Phys. Chem. Solids **39**, 1119 (1978).
[52] W. Ebeling, A. Feorster, V. E. Fortov, V. K. Gryaznov, and A. Y. Polishchuk, *Thermophysical Properties of Hot Dense Plasmas* (Teubner, Stutgart, 1991).
[53] R. Redmer, Electrical conductivity of dense metal plasmas, Phys. Rev. E **59**, 1073 (1999).
[54] S. D. Baalrud and J. Daligault, Effective Potential Theory for Transport Coefficients Across Coupling Regimes, Phys. Rev. Lett. **110**, 235001 (2013).
[55] S. D. Baalrud, and J. Daligault, Extending plasma transport theory to strong coupling through the concept of an effective interaction potential, Phys. Plasmas **21**, 055707 (2014).
[56] S. D. Baalrud and J. Daligault, Modified Enskog kinetic theory for strongly coupled plasmas, Phys. Rev. E **91**, 063107 (2015).
[57] P. Ludwig, H. Kählert, and M. Bonitz, Ion-streaming induced order transition in three-dimensional dust clusters, Plasma Phys. Control. Fusion **54**, 045011 (2012).
[58] P. Ludwig, W. J. Miloch, H. Kählert, and M. Bonitz, On the wake structure in streaming complex plasmas, New J. Phys. **14**, 053016 (2012).
[59] Hanno Kaehlert, Ion-dust streaming instability with non-Maxwellian ions, Phys. Plasmas **22**, 073703 (2015).
[60] G. I. Sukhinin and A. V. Fedoseev, Formation of a trapped-ion cloud around a dusty particle in low-density plasma, IEEE Trans. Plasma Sci. **38**, 2345 (2010).
[61] G. Lapenta, Dipole Moments on Dust Particles Immersed in Anisotropic Plasmas, Phys. Rev. Lett. **75**, 4409 (1995).
[62] T. S. Ramazanov, A. Zh. Gabdulin, and Zh. A. Moldabekov, Effect of dipole-dipole interaction on the compressional oscillations in two-dimensional Yukawa liquids, Contrib. Plasma. Phys. (2016) (to be published).
[63] K. I. Goledn, G. J. Kalman, P. Hartmann, and Z. Donko, Dynamics of two-dimensional dipole systems, Phys. Rev. E **82**, 036402 (2010).
[64] T. Ott, M. Stanley and M. Bonitz, Non-invasive determination of the parameters of strongly coupled 2D Yukawa liquids, Phys. Plasmas **18**, 063701 (2011).
[65] I. R. Yukhnovskiy and M. F. Golovko, *Static Theory of Classical Equilibrium Systems* (Naukova Dumka, Kiev, 1980).
[66] D. Else, R. Kompaneets, and S. V. Vladimirov, Shielding of a moving test charge in a quantum plasma, Phys. Rev. E **82**, 026410 (2010).
[67] R. Grassme and P. Bussemer, Friedel oscillations for temperatures $T \neq 0$, Phys. Lett. A **175**, 441 (1993).
[68] Lorin S. Matthews, Douglas A. Coleman, and Truell W. Hyde, Multipole expansions of aggregate charge: How far to go? *IEEE Transactions on Plasma Science* (IEEE, 2015), Vol. 44, pp. 519–524.
[69] J. Kaur, D. K. Nandy, B. Arora, and B. K. Sahoo, Properties of alkali-metal atoms and alkaline-earth-metal ions for an accurate estimate of their long-range interactions, Phys. Rev. A **91**, 012705 (2015).
[70] M. D. Kilgore, J. E. Daugherty, R. K. Porteous, and D. B. Graves, Ion drag on an isolated particulate in a low-pressure discharge, J. Appl. Phys. **73**, 7195 (1993).
[71] M. Belkhiri and M. Poirier, Analysis of density effects in plasmas and their influence on electron-impact cross sections, Phys. Rev. A **90**, 062712 (2014).
[72] C. Deutsch, N. A. Tahir, M. Barriga-Carrasco, V. Ceban, P. Fromy, D. Gilles, D. Leger, G. Maynard, B. Tashev, and L. Volpe, Multiple scattering in electron fluid and energy loss in multi-ionic targets, Nucl. Instrum. Methods Phys. Res. A **733**, 39 (2014).
[73] Young-Dae Jung, Anisotropic plasma effects on elastic electron-ion collisions in an anisotropic plasma, Phys. Scr. **71**, 303 (2005).
[74] W.-P. Hong and Y.-D. Jung, Influence of quantum diffraction and shielding on electron-ion collision in two-component semiclassical plasmas, Phys. Plasmas **22**, 012701 (2015).
[75] L. G. Stanton and M. S. Murillo, Ionic transport in high-energy-density matter, Phys. Rev. E **93**, 043203 (2016);
[76] D. Kremp, M. Schlanges, and W.-D. Kraeft, *Quantum Statistics of Nonideal Plasmas* (Springer, Berlin, 2005).

[77] G. Zwicknagel, C. Toepffer, and P. G. Reinhard, Stopping of heavy ions in plasmas at strong coupling, Phys. Rep. **309**, 117 (1999).
[78] P. E. Grabowski, M. P. Surh, D. F. Richards, F. R. Graziani, and M. S. Murillo, Molecular Dynamics Simulations of Classical Stopping Power, Phys. Rev. Lett. **111**, 215002 (2013).
[79] M.-J. Lee and Y.-D. Jung, Ion wake field effects on the dust-ion-acoustic surface mode in a semi-bounded Lorentzian dusty plasma, Phys. Plasmas **23**, 033702 (2016).